SCIENTIFIC REPORTS

OPEN

SUBJECT AREAS:
PHYSICAL CHEMISTRY
TWO-DIMENSIONAL MATERIALS

Received
31 December 2013

Accepted
5 March 2014

Published
25 March 2014

Correspondence and requests for materials should be addressed to W.W.L. (weiwei.lei@deakin.edu.au) or Y.C. (ian.chen@deakin.edu.au)

Template-Free Synthesis of Functional 3D BN architecture for removal of dyes from water

Dan Liu, Weiwei Lei, Si Qin & Ying Chen

Institute for Frontier Materials, Deakin University, Waurn Ponds, Victoria 3216, Australia.

Three-dimensional (3D) architectures are of interest in applications in electronics, catalysis devices, sensors and adsorption materials. However, it is still a challenge to fabricate 3D BN architectures by a simple method. Here, we report the direct synthesis of 3D BN architectures by a simple thermal treatment process. A 3D BN architecture consists of an interconnected flexible network of nanosheets. The typical nitrogen adsorption/desorption results demonstrate that the specific surface area for the as-prepared samples is up to 1156 $m^2 g^{-1}$, and the total pore volume is about 1.17 $cm^3 g^{-1}$. The 3D BN architecture displays very high adsorption rates and large capacities for organic dyes in water without any other additives due to its low densities, high resistance to oxidation, good chemical inertness and high surface area. Importantly, 88% of the starting adsorption capacity is maintained after 15 cycles. These results indicate that the 3D BN architecture is potential environmental materials for water purification and treatment.

Graphene, a two dimensional (2D) carbon sheet with one-atom thickness, has attracted increasing attention in recent years because of its unique structure and special properties[1–3]. As an analogue of graphene, boron nitride (BN) nanosheets possess a number of remarkable properties, including extremely high resistance to oxidation and good chemical inertness, electrical-insulating properties, high surface area, high thermal conductivity and stability[4–9]. Such outstanding properties make them especially promising in a wide range of applications such as field nanoemitters, photocatalyst, hydrogen storage, organic pollutant adsorption and clean-up of oil spillage[10–14]. Recently, many novel three-dimensional (3D) graphene assemblies have been synthesized by a number of different approaches[15–17]. These architectures of graphene are of interest in applications in electronics, catalysis devices, and sensors. Therefore, it is expected that developing 3D BN nanostructures will expand their significance in applications[18,19].

In recent years, water purification and treatment have drawn much attention due to the water crisis and the need for environmental protections. Organic dyes discharged from textiles, paper, plastics, tannery, and paint industries is considered as the primary pollutant in water sources[20,21]. Generally, the use of absorbent materials including active carbon, bioadsorbents and natural materials are considered to be a most desirable approach for the removal of dyes from water[22,23]. However, the low adsorption capacity and poor cycling capability have imposed significant challenges in employing them as primary adsorption materials to remove dyes from water. It has been demonstrated that BN nanomaterials can be used as an adsorption material for the removal of dyes from water[13,22]. The studies on the 3D BN architectures have flourished because they combine the property of BN materials and the stability of 3D nanostructure, which promise good adsorption capacity and stable cycling.

Herein we report the successful synthesis of a 3D BN architecture that combines high resistance to oxidation, good chemical inertness and high surface area. The 3D BN architecture with a cross-linked network structure is prepared by a simple thermal treatment process without the use of any catalyst or ex situ template. It affords a high adsorption capacity for organic dyes including cationic basic yellow 1 (BY) and anionic congo red (CR). More importantly, it can be easily recycled and reused by simply heating in air at 500°C after adsorption of dyes and up to 88% of the starting adsorption capacity is maintained after 15 cycles. This work may shed light on new adsorbent materials for the removal of dyes from water, and could potentially be applied in industrial processes for water purification and treatment.

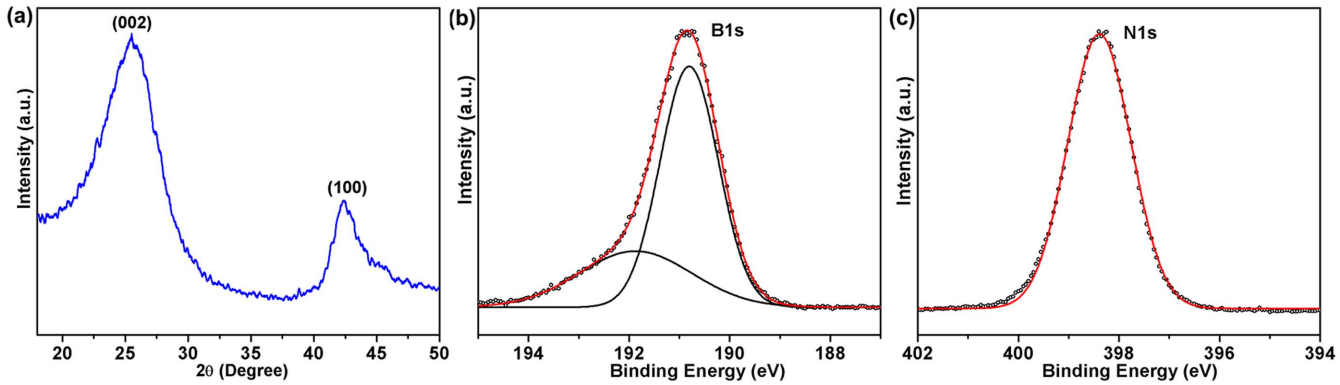

Figure 1 | XRD pattern (a), and XPS spectra: core-level B1s (b) and core-level N1s (c) of 3D BN architecture.

Results

The synthesis process of 3D BN architecture is descripted as below, boron trioxide (B_2O_3) and urea (CON_2H_4) with 1 : 10 molar ratio were first dissolved in methanol at room temperature. Urea was used as N source instead of guanidine hydrochloride in ref 14 due to the non-toxicity of urea. With the help of fast magnetic stirring, white crystalline powders were formed as methanol evaporated and dried out. The white crystal powders were heated in a tube furnace at 1000°C for 3 h under nitrogen/hydrogen (5% hydrogen) gas flow and white sample was produced. The excessive urea has an important role in the formation of 3D BN architecture. During the heating process, the urea is decomposed at high temperature releasing a number of gaseous species including CO_2, HCNO, N_2O, H_2O and NH_3[25]. The escape of gases (gas bubbles) acts as fugitive templates of the final porous structure.

The structure of the final products was studied by X-ray powder diffraction (XRD) firstly. According to the XRD pattern (Figure 1a), the sample has a typical hexagonal structure of *h*-BN with two broad diffraction peaks corresponding to the (002) and (100) planes, respectively. The chemical states of B and N elements were investigated using X-ray photoelectron spectroscopy (XPS). Figure 1b,c show typical B1s and N1s spectra, with corresponding binding energy of 190.8 eV, and 398.4 eV, respectively. These values are very close to the previously reported values of BN layers with BN_3 and NB_3 trigonal units[14,26]. The shoulder peak at 191.9 eV in the B1s spectrum is assigned to B-O bonds, which could result from the precursors and the exposure of the h-BN sample to air[14,26]. The B/N ratio from our XPS survey was calculated to be about 1.

The morphology of the sample was studied using scanning electron microscopy (SEM) and transmission electron microscopy (TEM). The SEM image in Figure 2a shows a typical 3D morphology of the BN samples. The enlarged views of the SEM images (Figure 2b,c) clearly reveal the interconnected network with the porous structure of the 3D BN architecture. The TEM image shown in Figure 2d is consistent with the SEM observations (Figure 2a–c). Both SEM and TEM images confirm that 3D BN architecture comprises hierarchical porous structure compared to BN nanosheets in ref 14, including macroporosity between the sheets (100–400 nm diameter), mesoporosity (2–20 nm) and microporosity (<2 nm) within the single nanosheets. The insert SAED pattern shows two characteristic diffraction rings corresponding to (002) and (100) lattice planes of BN, in consistent with the XRD result. In the high resolution TEM (HRTEM) images (Figure 2e,f), the porous structure (marked by the white arrows in the insert) and flat layer can be clearly observed, suggesting that the architecture structure is constructed by the curly and interconnected sheets. The HRTEM image in Figure 2f shows six parallel fringes at the edge region of the nanosheets, suggesting that the nanosheets have 6 stacked BN layers. The spacing between adjacent fringes was measured to be 0.34 nm which is close

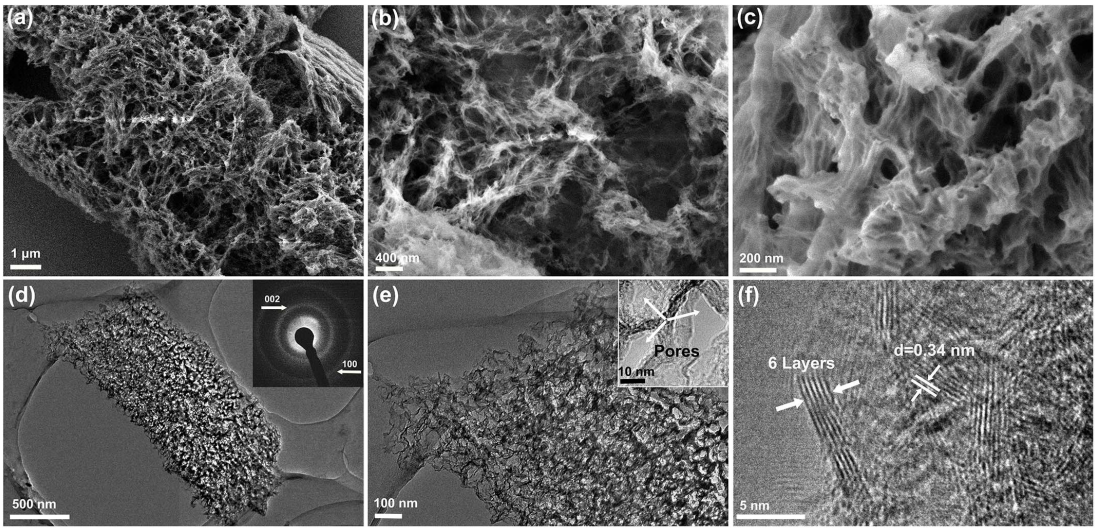

Figure 2 | (a) Low-magnification SEM image of the 3D BN architecture. (b,c) High-magnification SEM images revealing the interconnected network with the porous structure. (d) TEM image of a single 3D BN architecture, inserted SAED pattern indicating a layered BN structure. (e) HRTEM image of the architecture. The inset shows the typical porous structure. (f) HRTEM image of the edge folding of a nanosheet with 6 BN layers.

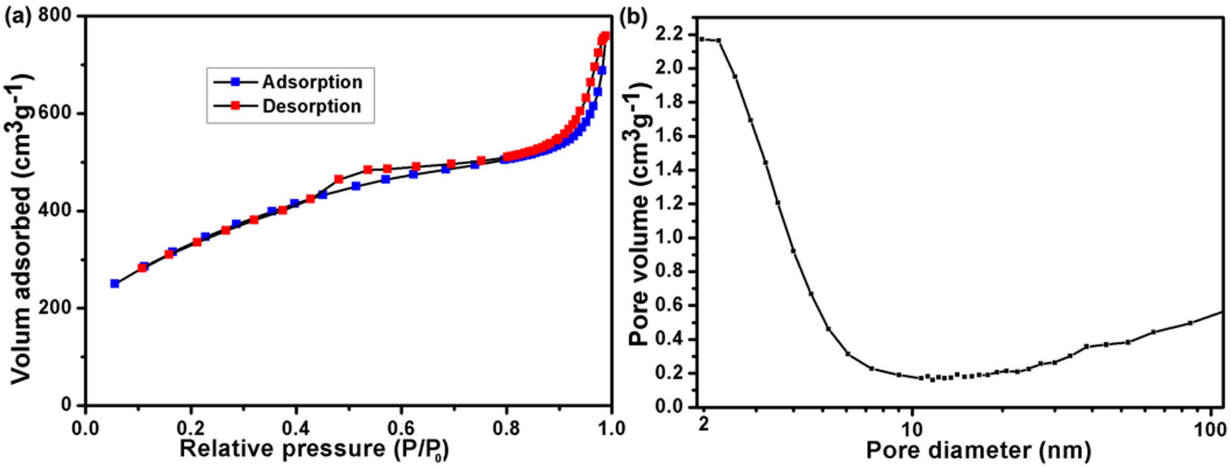

Figure 3 | **(a) Nitrogen adsorption–desorption isotherm and (b) corresponding pore size distributions of 3D BN architecture.**

to the (002) plane interdistance of *h*-BN. This is consistent with the result of the XRD.

The N_2 adsorption–desorption isotherms were conducted to determine the specific surface area of the 3D BN architecture. As shown in Figure 3a, the isotherms are a characteristic of type II isotherms with a hysteresis loop at a relative pressure between 0.4 and 1.0, which reveals predominant a mesoporous structure. Calculation with the BET model gives a specific surface area of 1156 m^2 g^{-1} and the total pore volumes 1.17 cm^3 g^{-1}. The pore diameters of the BN sample are around 2.5 nm and in the range of 2–10 nm (Figure 3b) evaluated by BJH method, which further confirm the results from SEM and TEM.

Discussion

Basic yellow 1 (BY), a textile dye (cationic) considered as a primary toxic pollutant in water resources, was chosen as a typical organic waste[27]. The starting BY concentration in water is 90 mg L^{-1}. The as-obtained 3D BN architecture can remove about 99% of the BY without any additives at room temperature, as shown by the photo of water extracted at different times in Figure 4a. UV-vis absorption spectroscopy was used to estimate the adsorption process at various absorption times of the BY solution after adding 10 mg of sample (Figure 4b). The characteristic absorption of BY at 412 nm was chosen for monitoring the adsorption process. After only 60 min, this peak became too weak to be observed, suggesting the high efficiency

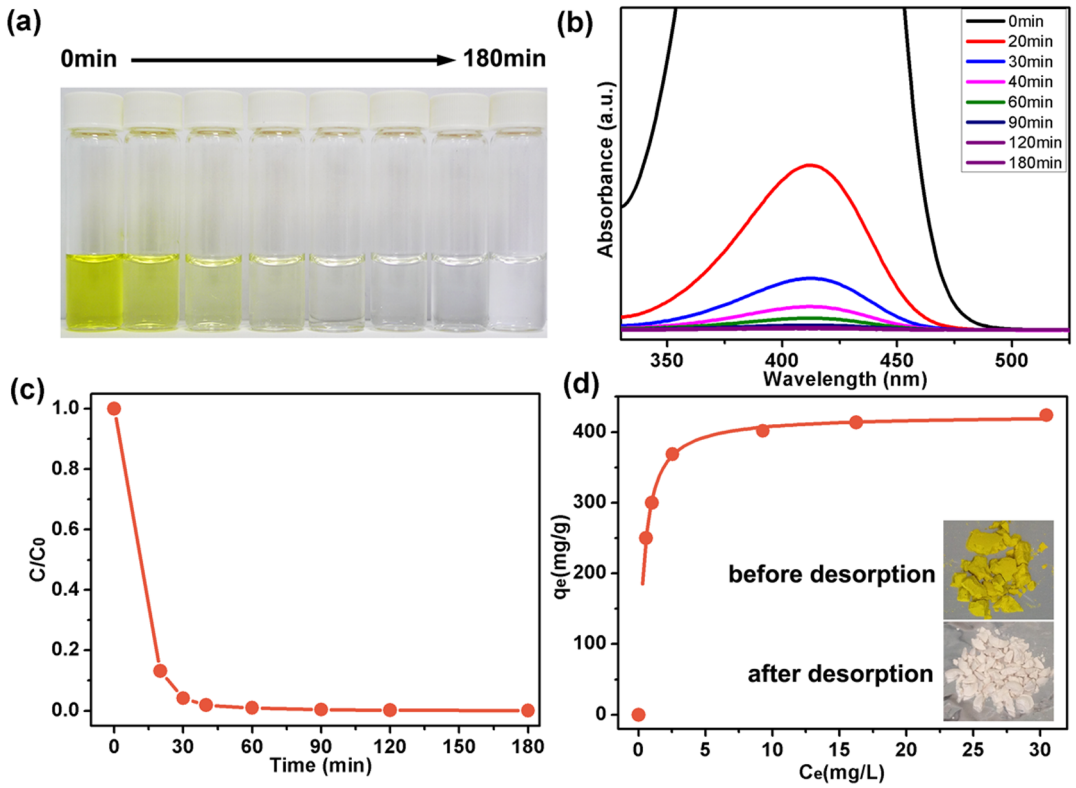

Figure 4 | (a) Photo of absorption progressof BY with time by new 3D BN architecture. (b) UV-vis absorption spectra of the aqueous BY solution (90 mg L^{-1}, 25 mL) in the presence of 3D BN architecture at different intervals, respectively. (c) Adsorption rates of the BY on 3D BN architecture. (d) Adsorption isotherms of BY on 3D BN architecture. The insets present the photographs of the 3D BN architecture with BY composites before (upper) and after (bottom) recovering by heating at 500°C for 2 h.

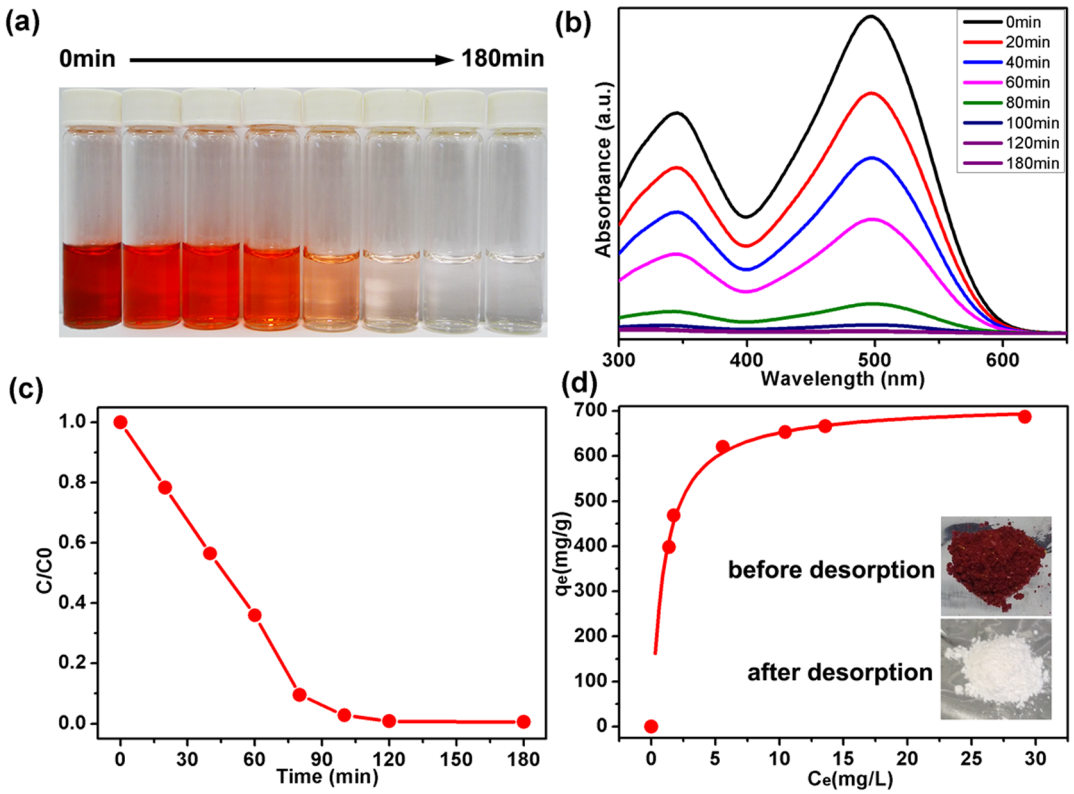

Figure 5 | (a) Photo of absorption progress of CR with time by new 3D BN architecture. (b) UV-vis absorption spectra of the aqueous CR solution (110 mg L^{-1}, 25 mL) in the presence of 3D BN architecture at different intervals, respectively. (c) Adsorption rates of the CR on 3D BN architecture. (d) Adsorption isotherms of CR on 3D BN architecture. The insets present the photographs of the 3D BN architecture with CR composites before (upper) and after (bottom) recovering by heating at 500°C for 2 h.

for BY removal. Figure 4b,c show about 99% of the BY can be removed from the water within 180 min without using any additives at room temperature.

Langmuir adsorption model is used to represent the relationship between the amount of dyes adsorbed at equilibrium (Q_e, mg g^{-1}) and the equilibrium solute concentration (C_e, mg L^{-1})[26]: $Q_e = Q_m bC_e/(1 + bC_e)$.

Where Q_m is the maximum adsorption capacity corresponding to complete monolayer coverage and b is the equilibrium constant (L mg^{-1}). The Langmuir isotherms represented in Figure 4d show the maximum adsorption capacity of 3D BN architecture to be 424.3 mg/g for BY (correlation coefficients, $R^2 > 0.99$).

Besides removing cationic BY, dyes with opposite charges commonly used in the textile industry, such as the anionic dye congo red (CR), can be removed from water with a high adsorption capacity by 3D BN architecture at room temperature, as shown by the photo and UV/Vis absorption curves at different times in Figure 5a–c, respectively. Figure 5d shows that the maximum adsorption capacity of CR is 717.5 mg g^{-1} ($R^2 > 0.99$). Both the calculated maximum adsorption capacities of BY and CR are significantly higher than those of most nanomaterials reported previously including BN hollow spheres, BN nanocarpets, MnO_2 hierarchical hollow nanostructures, $Ni(OH)_2$ and NiO nanosheets, Co_3O_4-Fe_3O_4 hollow spheres etc.[13,24,28–33].

The high adsorption capacities for dyes can be explained by the high specific surface area, highly hierarchical porous structure, and large pore volume of 3D BN architecture which provides the sufficient spaces for adsorbing dyes. Moreover, the electrostatic attraction between the boron nitride surface and the dyes species in solution is responsible for the dyes removal[13,24,34,35]. It is noted that a non-covalent interaction (such as π–π stacking interaction) exists between lamellar BN networks and aromatic rings, which is an important contribution for enhancing the adsorption of dye molecules on 3D BN architecture[13,24]. The reason could be due to the similarity of structural features of BN networks and the aromatic rings of organic dyes.

The stability and regeneration ability of adsorbents are key criteria for practical dyes removal applications. Herein, the BN containing dyes could be regenerated by easily heating at 500°C in air for 2 h (the inserted in Figure 4d and 5d). Figure 6 shows the reuse behavior of the BN sample upon BY removal/regeneration test for 15 cycles. As shown in Figure 6, the regenerated materials could retain almost the same adsorption performance after the second regenerations, and still remains over 88% after 15 cycles, indicating that the

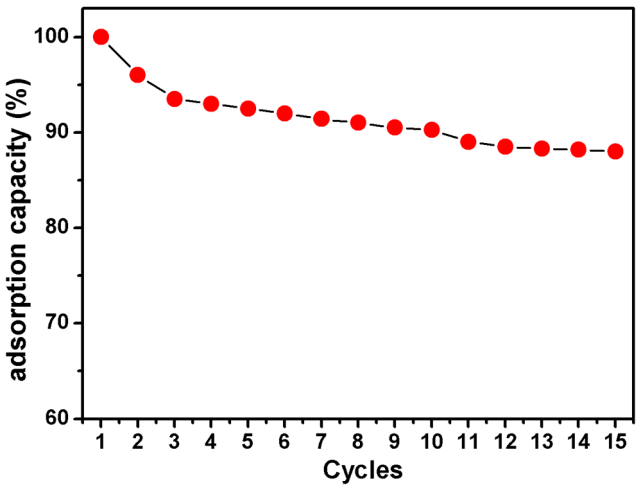

Figure 6 | **Adsorption capacity of BY on the 3D BN architecture in 15 successive cycles of desorption–adsorption (initial BY concentration: 250 mg L^{-1}; temperature: 25°C).**

as-prepared adsorbent has good reusability. The results clearly demonstrate the high stability and reuse capability of 3D BN, indicating its potentiality to be employed as efficient dyes adsorbents for practical use. Furthermore, it is worth noting that most adsorption results reported in the literature were obtained at optimal pH values. It is indicated that the high removal capacities probably could not be achieved at normal pH values under practical conditions. Thus, it is more indicative to estimate the potential capability of our 3D BN architecture for dyes removal in practical water purification, as it was measured directly, without the need for any pH adjustment.

In summary, we have synthesized 3D BN architecture constructed by porous nanosheets for high-performance removal of dyes from water, without any additives. The obtained 3D architecture is porous, high resistance to oxidation, good chemical inertness and light weight; it shows excellent adsorption performances for anionic and cationic dyes. Furthermore, it is highly stable and can be reused for several cycles without losing activity. All these features make the 3D BN architecture suitable for water purification, and indicate its potentiality in a wide range of applications including energy storage, hydrogen storage and capacitors.

Methods

In a typical synthesis, boron trioxide and urea with 1 : 10 molar ratio were mixed in 10 mL methanol under stirring to form a clear, colourless solution. After 24 h fast stirring, a white crystalline powder (a complex between the boron trioxide and urea) was formed. The resulting powders were put into quartz boat and then heated to 1000°C at a rate of 10°C min for 3 h under nitrogen/hydrogen (5% hydrogen) flow.

X-ray diffraction patterns of the sample were collected using a Panalytical X'Pert PRO diffraction system using Cu Kα radiation. The X-ray photoelectron spectra (XPS) were collected on an ESCALab MKII X-ray photoelectron spectrometer using non-monochromatized Mg-Ka X-ray as the excitation source. The structure of the sample was observed with a JEOL 2100F (operating at 200 kV) transmission electron microscope (TEM), and the scanning electron microscopic images were obtained with a Zeiss Supra 55 VP instrument. Nitrogen adsorption desorption isotherms were obtained using a Tristar 3000 apparatus at 77 K. The specific surface area was calculated by the Brunauer-Emmett-Teller (BET) method. The pore size distribution was calculated by the Barret-Joyner-Halenda (BJH) method.

Dye solutions (basic yellow 1 (BY) and congo red (CR)) of different concentrations were prepared by dissolving appropriate amounts of BY and CR into deionized water, respectively. In a typical adsorption of BY experiment, 10 mg of the as-prepared BN sample was added to 25 mL BY aqueous solution (90 mg L^{-1}) under stirring, and UV-vis adsorption spectra were recorded at 412 nm at different time intervals to monitor the process. The adsorption isotherm was obtained by varying the initial BY concentration. The adsorption studies of CR were similar to those of BY except for the difference in detection wavelength (496 nm for CR).

1. Li, X. S. *et al.* Large-area Synthesis of High-quality and Uniform Grapheme Films on Copper Foils. *Science* **324**, 1312–1314 (2009).
2. Sun, Z. Z. *et al.* Growth of Graphene from Solid Carbon Sources. *Nature* **468**, 549–552 (2010).
3. Li, X. H. *et al.* Metal-Free Activation of Dioxygen by Graphene/g-C3N4 Nanocomposites: Functional Dyads for Selective Oxidation of Saturated Hydrocarbons. *J. Am. Chem. Soc.* **133**, 8074–8077 (2011).
4. Zeng, H. B. *et al.* White Graphenes: Boron Nitride Nanoribbons via Boron Nitride Nanotube Unwrapping. *Nano Lett.* **10**, 5049–5055 (2010).
5. Chen, Z. G. *et al.* Novel boron nitride hollow nanoribbons. *ACS Nano* **2**, 2183–2191 (2008).
6. Song, L. *et al.* Large Scale Growth and Characterization of Atomic Hexagonal Boron Nitride Layers. *Nano Lett.* **10**, 3209–3215 (2010).
7. Zhi, C. Y. *et al.* Large-scale Fabrication of Boron Nitride Nanosheets and Their Utilization in Polymeric Composites with Improved Thermal and Mechanical Properties. *Adv. Mater.* **21**, 2889 (2009).
8. Gao, R. *et al.* High-yield Synthesis of Boron Nitride Nanosheets with Strong Ultraviolet Cathodoluminescence Emission. *J. Phys. Chem. C* **113**, 15160–15165 (2009).
9. Meng, X. L. *et al.* Low-Temperature Synthesis of Meshy Boron Nitride with a Large Surface Area. *Eur. J. Inorg. Chem.* **2010**, 3174–3178 (2010).
10. Zhu, Y. C., Bando, Y., Yin, L. W. & Golberg, D. Field nanoemitters: Ultrathin BN nanosheets protruding from Si_3N_4 nanowires. *Nano Lett.* **6**, 2982–2986 (2006).
11. Tang, C. C. *et al.* Improved TiO2 Photocatalytic Reduction by the Intrinsic Electrostatic Potential of BN Nanotubes. *Chem. Asian J.* **5**, 1220–1224 (2010).
12. Weng, Q. H. *et al.* Boron Nitride Porous Microbelts for Hydrogen Storage. *ACS Nano* **7**, 1558–1565 (2013).
13. Lian, G. *et al.* Controlled Fabrication of Ultrathin-shell BN Hollow Spheres with Excellent Performance in Hydrogen Storage and Wastewater Treatment. *Energy Environ. Sci.* **5**, 7072–7080 (2012).
14. Lei, W. W. *et al.* Porous Boron Nitride Nanosheets for Effective Water Cleaning. *Nature Comm* **4**, 1777 (2013).
15. Li, X. H. & Antonietti, M. Polycondensation of Boron- and Nitrogen-Codoped Holey Graphene Monoliths from Molecules: Carbocatalysts for Selective Oxidation. *Angew. Chem. Int. Ed.* **52**, 4572–4576 (2013).
16. Wu, Z. S. *et al.* 3D Nitrogen-Doped Graphene Aerogel-Supported Fe_3O_4 Nanoparticles as Efficient Electrocatalysts for the Oxygen Reduction Reaction. *J. Am. Chem. Soc.* **134**, 9082–9085 (2012).
17. Ji, H. X. *et al.* Ultrathin graphite foam: a three-dimensional conductive network for battery electrodes. *Nano Lett.* **12**, 2446–2451 (2012).
18. Alauzun, J. G. *et al.* Novel monolith-type boron nitride hierarchical foams obtained through integrative chemistry. *J. Mater. Chem.* **21**, 14025–14030 (2011).
19. Schlienger, S. *et al.* Micro-, Mesoporous Boron Nitride-Based Materials Templated from Zeolites. *Chem. Mater.* **24**, 88–96 (2012).
20. Robinson, T., McMullan, G., Marchant, R. & Nigam, P. Remediation of Dyes in Textile Effluent: a Critical Review on Current Treatment Technologies with a Proposed Alternative. *Bioresour. Technol.* **77**, 247–255 (2001).
21. Forgacs, E., Cserháti, T. & Oros, G. Removal of Synthetic Dyes from Wastewaters: a Review. *Environ. Int.* **30**, 953–971 (2004).
22. Crini, G. Non-conventional Low-cost Adsorbents for Dye Removal: a Review. *Bioresour. Technol.* **97**, 1061–1085 (2006).
23. Rafatullah, M., Sulaiman, O., Hashim, R. & Ahmad, A. Adsorption of Methylene Blue on Low-cost Adsorbents: a Review. *J. Hazard. Mater.* **177**, 70–80 (2010).
24. Zhang, X., Lian, G., Zhang, S. J., Cui, D. L. & Wang, Q. L. Boron nitride nanocarpets: controllable synthesis and their adsorption performance to organic pollutants. *CrystEngComm* **14**, 4670–4676 (2012).
25. Oxley, J. C., Smith, J. L., Naik, S. & Moran, J. Decompositions of Urea and Guanidine Nitrates. *J. Ener. Mater.*, **27**, 17–39 (2009).
26. Lei, W. W., Portehault, D., Dimova, R. & Antonietti, M. Boron carbon nitride nanostructures from salt melts: tunable water-soluble phosphors. *J. Am. Chem. Soc.* **133**, 7121–7127 (2011).
27. Wang, B. *et al.* Template-free formation of uniform urchin-like α-FeOOH hollow spheres with superior capability for water treatment. *Adv. Mater.* **24**, 1111–1116 (2012).
28. Fei, J. B. *et al.* Controlled preparation of MnO_2 hierarchical hollow nanostructures and their application in water treatment. *Adv. Mater.* **20**, 452–456 (2008).
29. Cheng, B., Le, Y., Cai, W. Q. & Yu, J. G. Synthesis of hierarchical $Ni(OH)_2$ and NiO nanosheets and their adsorption kinetics and isotherms to Congo red in water. *J. Hazard. Mater.* **185**, 889–897 (2011).
30. Wang, X. *et al.* Multishelled Co_3O_4-Fe_3O_4 hollow spheres with even magnetic phase distribution: Synthesis, magnetic properties and their application in water treatment. *J. Mater. Chem.* **21**, 17680–17687 (2011).
31. Yang, Z. J. *et al.* Mesoporous CeO_2 Hollow Spheres Prepared by Ostwald Ripening and Their Environmental Applications. *Eur. J. Inorg. Chem.* **2010**, 3354–3359 (2010).
32. Yu, C. C. *et al.* Template-free Preparation of Mesoporous Fe_2O_3 and its Application as Absorbents. *J. Phys. Chem. C* **112**, 13378–13382 (2008).
33. Fei, J. B. *et al.* Large-scale Preparation of 3D Self-assembled Iron Hydroxide and Oxide Hierarchical Nanostructures and Their Applications for Water Treatment. *J. Mater. Chem.* **21**, 11742–11746 (2011).
34. Zhong, L. S. *et al.* Self-Assembled 3D Flowerlike Iron Oxide Nanostructures and Their Application in Water Treatment. *Adv. Mater.* **18**, 2426–2431 (2006).
35. Liang, H. W. *et al.* Robust and Highly Efficient Free-Standing Carbonaceous Nanofiber Membranes for Water Purification. *Adv. Funct. Mater.* **21**, 3851–3858 (2011).

Acknowledgments

Financial support from the Australian Research Council Discovery Program, the Australian Research Council Discovery Early Career Researcher Award scheme, and Deakin University, Central Research Grant Scheme are acknowledged.

Author contributions

D.L. conceived the project. D.L., W.W.L., S.Q. and Y.C. designed the experiments. D.L., W.W.L. and S.Q. synthesized the BN architecture and performed the experiments. All authors contributed to analyses the data and discussions regarding the research. D.L. wrote the manuscript.

Additional information

Competing financial interests: The authors declare no competing financial interests.

How to cite this article: Liu, D., Lei, W.W., Qin, S. & Chen, Y. Template-Free Synthesis of Functional 3D BN architecture for removal of dyes from water. *Sci. Rep.* **4**, 4453; DOI:10.1038/srep04453 (2014).